CONF-750806--4

PIPE BLOWDOWN ANALYSES USING EXPLICIT NUMERICAL SCHEMES

BY

Robert W. Lyczkowski

Robert A. Grimesey

and

Charles W. Solbrig

Aerojet Nuclear Company*
Idaho Falls, Idaho 83401

A Paper Submitted to the Session, "Heat Transfer in Reactor Safety", 15th National Heat Transfer Conference, San Francisco, August 10-13, 1975.

* Prepared for the U.S. Nuclear Regulatory Commission

ABSTRACT

Several explicit numerical schemes were investigated to solve the homogeneous equations of change for one-dimensional fluid flow and heat transfer. The most successful technique investigated is the alternating gradient method which is based on the two-step Lax-Wendroff procedure. Agreement with experimental results is very good.

CONTENTS

Abstract i

1. Introduction 1

2. Considerations in the Selection of a Numerical Scheme for Blowdown Calculations 3

3. Basic Equations 8

4. Description of the LW and AGM Numerical Schemes 9

5. Basic Difference Equations and Solution Sequence 14

   5.1 First Cycle 14

   5.2 Second Cycle 16

6. Initial and Boundary Conditions 18

   6.1 Inlet Boundary, v>0 20

   6.2 Inlet Boundary, v = 0 21

   6.3 Outlet Boundary, v>0 22

   6.4 Flow Reversal at an Outflow Boundary 24

7. Stability Analyses of the Alternating Gradient Method 25

8. Truncation Error of the AGM and LW Schemes 29

9. Results of Computations 31

10. Conclusions 42

11. References 44

FIGURES

Figure 1 - Illustration of the Alternating Gradient Method 11

Figure 2 - Two-Dimensional Alternating Gradient Method 13

Figure 3 - Comparison of the Lax-Wendroff and Alternating Gradient Methods with the Theoretical Solution 33

Figure 4 - Ideal Gas Blowdown Pressure Results 34

Figure 5 - Ideal Gas Blowdown Velocity Results 35

Figure 6 - Comparison of Alternating Gradient Short Term Pressure Transient Computations with Edwards' Data 38

Figure 7 - Comparison of Alternating Gradient Long Term Pressure Transient Response Computations with Edwards' Data. . . . 39

Figure 8 - Comparisons of Alternating Gradient Code Results with Edwards' Data for Volume Fraction Steam Transient 40

INTRODUCTION

The loss-of-coolant accident is a hypothetical transient in a nuclear power reactor which must be designed for before such a reactor can be licensed. The heat transferred to the coolant in the system is the major factor in determining whether the reactor could satisfactorily withstand such an accident. The accurate prediction of the velocity and temperature of the coolant during a hypothetical loss-of-coolant accident is essential to predicting the heat transfer. Many computer programs which are used for these calculations are based on equal phase velocity, equal phase temperature (EVET) theories for the calculation of the fluid velocity and temperature.(For example, Moore and Rettig, 1973). Most of these programs use an implicit solution scheme to solve the fluid continuity, momentum, and energy equations. In addition, the continuity and energy equations are solved at certain positions (control volumes) and the momentum equations are solved at other locations (junctions). This technique is referred to here as the displaced mesh scheme. As part of a continuing effort to improve the current computational methods, several studies were conducted to determine the advantages of other solution schemes. The results of the study of explicit numerical schemes are presented here. Sample one-dimensional results which were obtained with two of these methods are presented and compared with analytical solutions and experimental results.

The results obtained were solutions to three different problems. The first solution is for a shock tube problem which tests the adequacy of a basic finite difference scheme on the interior because boundary

conditions are not involved. The second solution involves the history of a perfect gas being expelled from a straight pipe with one end open. This problem tests the adequacy of a numerical scheme to handle boundary conditions. The third solution involves the expulsion of a two phase mixture from a pipe. This problem tests the adequacy of both the finite difference scheme and the boundary conditions to describe the behavior of a complex fluid. This latter solution was compared with experimental results (Edwards and O'Brien, 1970).

2. CONSIDERATIONS IN THE SELECTION OF A NUMERICAL SCHEME FOR BLOWDOWN CALCULATIONS

The equations which are of interest in this paper are systems of hyperbolic equations in the form

$$\frac{\partial V}{\partial t} + \frac{\partial F(V)}{\partial x} = G \tag{1}$$

where V and G are vectors and F is a vector function. These equations may be rewritten as

$$\frac{\partial V}{\partial t} + A \frac{\partial V}{\partial x} = G \tag{2}$$

where A is a matrix which is the Jacobian of F with respect to V.

The numerical solution schemes of interest in this paper are explicit. An explicit solution technique allows each quantity to be solved for individually. Implicit solutions involve the solution of simultaneous algebraic equations. The solution of these algebraic equations is usually carried out with an iteration scheme which can often be shown to be equivalent in the amount of computer time involved to advance additional time steps in an explicit solution. For slow transients, the large time step often allowed with implicit schemes combined with the number of iterations results in less computer

time than the use of explicit schemes. For fast transients, explicit schemes are often the faster of the two methods because the step is restricted by the velocity as is illustrated in the following.

The usual stability restriction associated with explicit solutions for one-dimensional fluid flow is

$$(|v| + c)\frac{\Delta t}{\Delta x} \leq 1 \tag{3}$$

where v is the velocity and c is the speed of sound.

Implicit solutions are often free of stability restrictions in subsonic flow but accuracy of the solution requires that

$$v\ \frac{\Delta t}{\Delta x} \leq 1 \tag{4}$$

Restriction 4 is usually much less severe in the subsonic case than Restriction (3). However, when the speed of the fluid is close to sonic, these restrictions are very close. In this instance, the explicit solution requires less work because no iterations are required. Since the blowdown solution of interest in this paper involves high flow speeds, and since the speed of sound can be very low for a two phase mixture, explicit schemes were used for this study. Explicit schemes have the additional advantage that they are much easier to program than implicit solutions.

Many of the explicit numerical schemes have been used to solve shock tube problems (Roach, 1972). The blowdown problem is different than the shock tube problem in at least two respects; boundary conditions and steam tables. The boundary conditions are of vital interest in the blowdown problem because they significantly affect the pressure and mass in the system. The boundary conditions in the shock tube problem are insiginificant because the boundaries are not reached. The blowdown problem uses water-steam properties which are much more complicated than the perfect gas properties frequently used in the shock tube solution. The pressure must be calculated from the equation of state in an explicit scheme if the equation is not linear or linearized in an explicit scheme. This calculation is very sensitive in the all-liquid region.

Explicit schemes using the displaced mesh were investigated in this study. They were found to be unsatisfactory for the blowdown problem because the density, ρ, the energy, U, and the velocity, v, are solved for at different points. The density always decreases near the exit whereas the velocity increases. Use of an average for these quantities to obtain the ρv, ρv^2, and ρvU products always resulted in the incorrect calculation of spatial derivatives of one or more of these products. These calculations resulted in mass, energy, and momentum imbalances near the exit which caused the velocity to eventually become unstable. Coincident mesh schemes to be described in this paper yield satisfactory calculations.

Most of the explicit numerical schemes involve three spatial points. A lesser number of points is desirable. A numerical scheme which involves only two points is

$$\frac{V_i^{n+1} - V_i^n}{\Delta t} + A_i^n \frac{V_i^n - V_{i-1}^n}{\Delta x} = G_i^n \tag{5}$$

The fewer points are desirable because information is propagated more rapidly than possible physically if more points are involved. Fewer points also require fewer boundary conditions. The disadvantages of this scheme seem to outweigh the advantages, however. The spatial derivative is not symmetric which can lead to biasing errors. The scheme is not stable for negative velocities. Negative velocities can be handled by changing the spatial derivative to

$$\frac{V_i^{n+1} - V_i^n}{\Delta t} + A_i^n \frac{V_{i+1}^n - V_i^n}{\Delta x} = G_i^n \tag{6}$$

However, treating both positive and negative velocities in the same calculation involves matching of Equations (5) and (6) at the points where the velocity changes sign.

Use of a symmetric spatial derivative yields the following scheme

$$\frac{V_i^{n+1} - V_i^n}{\Delta t} + A_i^n \frac{V_{i+1}^n - V_{i-1}^n}{2\Delta x} = G_i^n \tag{7}$$

This finite difference scheme is unconditionally unstable (Lax, 1954). A slight variant of this scheme which is conditionally stable can be obtained by the approximation

$$V_i^n = \tfrac{1}{2}\,(V_{i+1}^n + V_{i-1}^n)$$

to obtain

$$\frac{V_i^{n+1} - \tfrac{1}{2}\left(V_{i+1}^n + V_{i-1}^n\right)}{\Delta t} + A_i^n \frac{V_{i+1}^n - V_{i-1}^n}{2\Delta x} = G_i^n \qquad (8)$$

This scheme is known as the basic Lax method (Lax, 1954). It forms the basis for the two-step Lax-Wendroff scheme (Richtmyer and Morton, 1967) and the alternating gradient method presented in this paper. One difficulty with the Lax method is in the extension to two dimensions. The value at the old time is replaced by an average of four values. A one-dimensional problem solved with the two-dimensional version will not yield the same results as the same problem solved with the one-dimensional scheme.

3. BASIC EQUATIONS

The basic equations which are solved in this paper are one-dimensional equations of change with friction and heat transfer for horizontal flow in a tube. These are

continuity

$$\frac{\partial \rho}{\partial t} + \frac{\partial \rho v}{\partial x} = 0 \tag{9}$$

momentum

$$\frac{\partial \rho v}{\partial t} + \frac{\partial \rho v^2}{\partial x} + \frac{\partial P}{\partial x} + F = 0 \tag{10}$$

where $F = f_f \rho |v| \, v/2D_h$

P = pressure

f_f = Moody friction factor

D_h = hydraulic diameter

energy

$$\frac{\partial \rho U}{\partial t} + \tfrac{1}{2} \frac{\partial \rho v^2}{\partial t} + \frac{\partial \rho v U}{\partial x} + \tfrac{1}{2} \frac{\partial \rho v^3}{\partial x} + \frac{\partial v P}{\partial x} = Q \tag{11}$$

where Q = the heat transfer rate

U = the internal energy

4. DESCRIPTION OF THE LW AND AGM NUMERICAL SCHEMES

The two numerical schemes which were used to generate results presented in this paper are discussed in this section. These two schemes are the alternating gradient method (AGM) and the two-step Lax-Wendroff (LW) method. The latter method has been developed in detail in Richtmyer and Morton (1967, p 300). It will only be described here in terms of the difference between it and the AGM.

The alternating gradient method derives its name from the numerical scheme which is a two step method with predictor and corrector equations. The predictor evaluates the spatial gradients at the old time to predict the desired information at the new time. The corrector estimates the spatial gradients at the new time.

The numerical scheme can be illustrated by considering the equations of change in the form of Equation (1) with

$$V = \begin{bmatrix} \rho \\ m \\ E \end{bmatrix} \qquad F(V) = \begin{bmatrix} m \\ (m^2/\rho) + P \\ (E+P)\ m/\rho \end{bmatrix} \qquad G = \begin{bmatrix} 0 \\ -F \\ Q \end{bmatrix} \tag{12}$$

where $m = \rho v$

and $E = U + \frac{1}{2}v^2$

The pressure is given by the equation of state

$$P = P_{eos}\ (\rho, U) \tag{13}$$

The predictor step calculates provisional values at the new time at midpoints between the final points with the equation

$$\hat{V}^{n+1}_{j+\frac{1}{2}} = \frac{1}{2}\left(V^n_{j+1} + V^n_j\right) - R_x\left(F^n_{j+1} - F^n_j\right) + \Delta t\frac{1}{2}\left(G^n_{j+1} + G^n_j\right) \tag{14}$$

where F^n_j is an abbreviation for $F\left(V^n_j\right)$

$R_x = \Delta t/\Delta x$

The final values are calculated by the corrector equation which uses the provisional values obtained from the predictor to estimate the spatial gradients. The corrector is given as

$$V^{n+1}_j = V^n_j - R_x\left(\hat{F}^{n+1}_{j+\frac{1}{2}} - \hat{F}^{n+1}_{j-\frac{1}{2}}\right) + \Delta t G^n_j \tag{15}$$

where $\hat{F}^n_j$ is an abbreviation for $F\left(\hat{V}^{n+1}_j\right)$

This numerical scheme is completely explicit because no quantities need be solved for simultaneously. It is illustrated in Figure 1. The predictor is shown as a dashed line and the corrector is shown as a solid line. The alternating gradient method can be modified to an implicit scheme by calculating $\hat{V}^{n+1}_{j+\frac{1}{2}}$ and $\hat{V}^{n+1}_j$ for all points which lie in the calculational region with the predictor, calculating V^{n+1}_j and $V^{n+1}_{j+\frac{1}{2}}$ for all points in the region with the corrector, and then reapplying the corrector until a converged answer is obtained.

The two-step Lax-Wendroff method differs from the AGM method in that it calculates the values $V_{j+1/2}^{n+1}$ in the first step and uses these values to estimate the spatial gradient in the second step. The two step Lax-Wendroff method cannot be made implicit by continued application of the second equation and thus basically differs from the AGM.

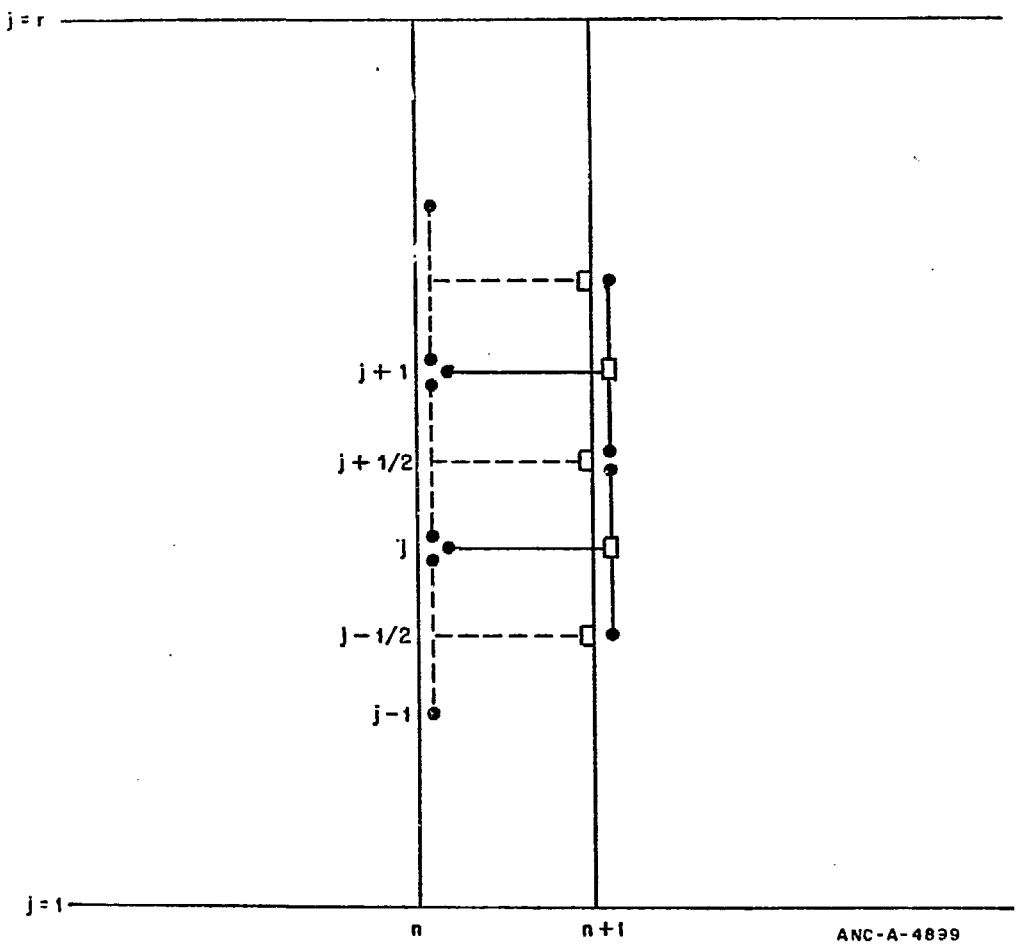

Figure 1. Illustration of the Alternating Gradient Method

The two-step Lax-Wendroff scheme and the alternating gradient method treat all the equations with the same numerical technique. These methods differ from the numerical methods currently used in Loss-of-Coolant Accident codes such as RELAP4 (Moore and Rettig, 1973), FLASH4 (Porshing, et al., 1971). RELAP4 and FLASH4 are implicit codes which use different methods to treat each equation.

Both the two-step Lax-Wendroff method and the alternating gradient method can be extended to multidimensions. For two dimensions the tentative values $\hat{V}^{n+1}_{j+\frac{1}{2},k}$ and $\hat{V}^{n+1}_{j,k+\frac{1}{2}}$ for all points within the region are calculated with the predictor equation, and the final values at the new time $V^{n+1}_{j,k}$ and $V^{n+1}_{j+\frac{1}{2},k+\frac{1}{2}}$ for all points within the region are calculated with the corrector equation. This procedure is illustrated in Figure 2. The tentative values are calculated at the new time at the points marked by Xs and the final values are calculated at the points marked by •s. The small square indicates the point which can be calculated at the new time by the other points marked by •s and known at the previous time.

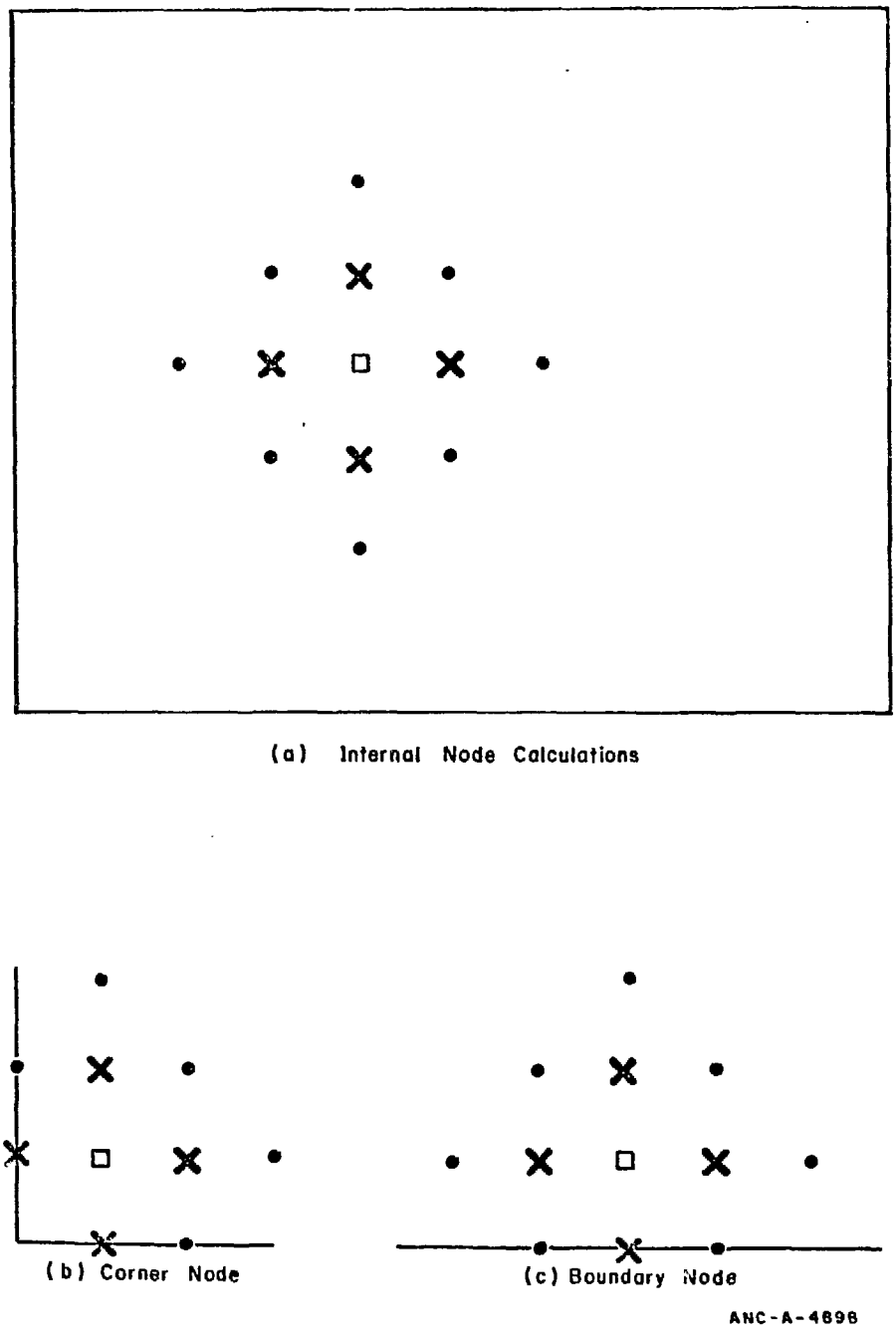

Figure 2. Two-Dimensional Alternating Gradient Method

5. BASIC DIFFERENCE EQUATIONS AND SOLUTION SEQUENCE

The alternating gradient method as applied to the continuity, momentum, and energy equations is described in this section. The boundary conditions are described in the following section:

5.1 First Cycle. Predictor Solution

The predictor, Equation (14), is applied respectively to the momentum, continuity, and the energy equation

1) The predictor form of the momentum equation is solved for the ρv product

$$(\widehat{\rho v})^{n+1}_{j+\frac{1}{2}} = \tfrac{1}{2}\left[(\rho v)^n_{j+1} + (\rho v)^n_j\right] - R_x\left[(\rho v^2)^n_{j+1} - (\rho v^2)^n_j\right] - R_x(P^n_{j+1} - P^n_j) - \frac{\Delta t}{2}(F^n_{j+1} + F^n_j) \tag{16}$$

2) The continuity equation is solved for ρ

$$\hat{\rho}^{n+1}_{j+\frac{1}{2}} = \tfrac{1}{2}(\rho^n_{j+1} + \rho^n_j) - R_x\left[(\rho v)^n_{j+1} - (\rho v)^n_j\right] \tag{17}$$

The velocity is then computed from ρv and ρ

$$\hat{v}^{n+1}_{j+\frac{1}{2}} = \frac{\widehat{\rho v}^{n+1}_{j+\frac{1}{2}}}{\rho^{n}_{j+\frac{1}{2}}} \tag{18}$$

3) The energy equation is solved for the ρU product

$$(\widehat{\rho U})^{n+1}_{j+\frac{1}{2}} = -\tfrac{1}{2}(\widehat{\rho v^2})^{n+1}_{j+\frac{1}{2}} + \tfrac{1}{2}\left[\rho_{j+1}\,(U_{j+1} + \tfrac{1}{2}v^2_{j+1}) + \rho_j(U_j + \tfrac{1}{2}v^2_j)\right]^n$$

$$- R_x\left[(\rho vU)^n_{j+1} - (\rho vU)^n_j\right] - \frac{R_x}{2}\left[(\rho v^3)^n_{j+1} - (\rho v^3)^n_j\right] - R_x\left[vp^n_{j+1} - vp^n_j\right] \tag{19}$$

$$+ \frac{\Delta t}{2}\left[\dot{Q}^n_{j+1} + \dot{Q}^n_j\right]$$

The internal energy is computed from $\widehat{\rho U}$ and $\hat{\rho}$

$$\hat{U}^{n+1}_{j+\frac{1}{2}} = \frac{(\widehat{\rho U})^{n+1}_{j+\frac{1}{2}}}{\rho^{n+1}_{j+\frac{1}{2}}} \tag{20}$$

4) The tentative pressure is solved for from the equation of state

$$\hat{p}^{n+1}_{j+\frac{1}{2}} = p_{eos}\,(\hat{\rho}^{n+1}_{j+\frac{1}{2}},\ \hat{U}^{n+1}_{j+\frac{1}{2}}) \tag{21}$$

5.2 Second Cycle. Corrector Solution

The corrector, Equation (15), is applied to the equations of change in the same order as the predictor.

1) The corrector equation is solved for ρv

$$(\rho v)_j^{n+1} = \rho_j^n v_j^n - R_x\left[(\hat{\hat{\rho v^2}})_{j+\frac{1}{2}}^{n+1} - (\hat{\hat{\rho v^2}})_{j-\frac{1}{2}}^{n+1}\right] - R_x\,(\hat{P}_{j+\frac{1}{2}} - \hat{P}_{j-\frac{1}{2}})^{n+1} - \Delta t\, F_j^n \qquad (22)$$

2) The continuity equation is then solved for the density ρ

$$\rho_j^{n+1} = \rho_j^n - R_x\left[(\widehat{\rho v})_{j+\frac{1}{2}}^{n+1} - (\widehat{\rho v})_{j-\frac{1}{2}}^{n+1}\right] \qquad (23)$$

The velocity is computed from

$$v_j^{n+1} = \frac{(\rho v)_j^{n+1}}{\rho_j^{n+1}} \qquad (24)$$

3) The energy equation is solved for the ρU product

$$(\rho U)_j^{n+1} = -\tfrac{1}{2}(\rho_j v_j^2)^{n+1} + \rho_j^n U_j^n + \tfrac{1}{2}(v_j^2)^n - R_x\left[(\hat{\hat{\rho v U}})_{j+\frac{1}{2}}^{n+1} - (\hat{\hat{\rho v U}})_{j-\frac{1}{2}}^{n+1}\right]$$

$$\frac{R_x}{2}\left[(\hat{\hat{\rho v^3}})_{j+\frac{1}{2}}^{n+1} - (\hat{\hat{\rho v^3}})_{j-\frac{1}{2}}^{n+1}\right] - R_x\left[(\hat{\hat{vP}})_{j+\frac{1}{2}}^{n+1} - (\hat{\hat{vP}})_{j-\frac{1}{2}}^{n+1}\right] + \Delta t Q_j^n \qquad (25)$$

The internal energy is computed from

$$U_j^{n+1} = \frac{(\rho U)_j^{n+1}}{\rho_j^{n+1}} \tag{26}$$

4) The pressure is calculated from the equation of state

$$P_j^{n+1} = P_{eos}(\rho_j^{n+1}, U_j^{n+1}) \tag{27}$$

6. INITIAL AND BOUNDARY CONDITIONS

The initial conditions which are prescribed include the internal energy, pressure, and velocity. The density is determined from the equation of state. These values are not specified at the tentative locations (that is, at the points which include a 1/2 in the spatial index). The initial conditions are specified at time zero as

$$\begin{aligned} U_i^1 &= \text{UIC}\ (x_i) \\ p_i^1 &= \text{PIC}\ (x_i) \\ v_i^1 &= \text{VIC}\ (x_i) \\ \rho_i^1 &= \rho_{eos}\ (\text{UIC}\ (x_i),\ \text{PIC}\ (x_i)) \end{aligned} \tag{28}$$

where UIC, PIC, VIC are specified functions and ρ_{eos} is the density form of the equation of state. These initial conditions are also specified at the boundaries at the initial time.

Experience has shown that the density, energy, and pressure are best specified in agreement with the equation of state rather than independently. The restrictions which must be placed on the relationship between the other variables is not well understood. An example which involves incompressible flow illustrates that some restrictions must exist. If an incompressible liquid flow rate in one dimension is to be computed, the pressure drop must be specified as zero for compatibility in the horizontal frictionless case. No similar restriction is known to apply in the compressible problem. No difficulty was encountered in applying the initial conditions specified by Equation (28) for the solutions obtained in this paper.

The boundary conditions as applied involve quantities only at the full node points (points which have an integral number in the spatial index) and do not involve any tentative locations. The treatment of boundary conditions has received far less study in the literature and less is known about these conditions than numerical schemes used on the interior. Accuracy studies on boundary conditions have been performed and are presented in the literature for some numerical schemes. Chen (1973) analyzed the one-dimensional shallow water wave equations, Nitta (1962) studied a single advective equation, Matsuno (1966) investigated false reflections at boundaries, and Chu and Sereny (1974) analyzed several gas dynamics problems using the two-step Lax-Wendroff numerical procedure.

The numerical schemes are often of a higher order than the differential equations. When the numerical scheme is of a higher order, more boundary conditions are required for the partial difference equations than for the partial differential equations. The additional conditions are referred to as missing boundary conditions. This circumstance occurs with both the two-step Lax-Wendroff and the alternating gradient methods. The theory of characteristics applied to the differential equations restricts the boundary conditions which may be specified. The boundary conditions which are considered in this paper represent inflow, outflow, and closed boundary conditions. Missing boundary conditions only occur for the outflow boundary. The boundary information which is missing is the internal energy at the outflow boundary. This additional information is obtained by extrapolating from the interior.

The general boundary conditions for inlet flow, outlet flow, and closed boundaries available in both the LW and AGM schemes are presented in this section. The basic boundary data that can actually be specified (prescribed) in the code are pressure, energy, and velocity. At an inflow boundary, the theory of characteristics permits only two items to be specified, U and p or v, and for an outflow boundary only one item can be specified, p or v. Nothing except a zero velocity may be specified at a closed boundary. Specified inlet and outlet velocity conditions except zero are not discussed in this paper. The index notation is defined in Figure 1. The boundary at j = 1 is arbitrarily treated as an inlet boundary and the boundary at j = r is treated as an outlet boundary in the following discussion.

6.1 Inlet Boundary, v>0

The internal energy

$$U_1^{n+1} = UI\ (t^{n+1}) \tag{29}$$

is always specified at an inlet boundary.

The pressure is prescribed as a function of time as

$$p_1^{n+1} = PI\ (t^{n+1}) \tag{30}$$

Since the pressure is specified at the boundary, the velocity can be determined from the ρv product in the momentum equation and from the density in the continuity equation at the boundary.

The form of the momentum equation used is

$$(\rho v)_1^{n+1} = (\rho v)_1^n - R_x \left[(\rho v^2)_2^{n+1} - (\rho v^2)_1^n\right] - R_x \left[p_2^{n+1} - p_1^{n+1}\right] - \Delta t \, F_1^n \quad (31)$$

The density is determined from the continuity equation written with a nonsymmetric space derivative

$$\rho_1^{n+1} = \rho_1^n - R_x\left[(\rho v)_2^{n+1} - (\rho v)_1^{n+1}\right] \quad (32)$$

Then the new velocity at the boundary is computed from

$$v_1^{n+1} = \frac{(\rho v)_1^{n+1}}{\rho_1^{n+1}} \quad (33)$$

6.2 Inlet Boundary, v = 0

When the velocity is zero at a boundary (closed end), no other conditions can be prescribed. The density, pressure, and energy may be determined from the equations of change.

The density is first obtained from the continuity equation. The continuity equation with $v = 0$ is

$$\frac{\partial \rho}{\partial t} = -\rho \frac{\partial v}{\partial x} \quad (34)$$

In finite difference form, Equation (34) becomes

$$\rho_1^{n+1} = \rho_1^n - \rho_1^{n+1} R_x v_2^{n+1}$$

or

$$\rho_1^{n+1} = \frac{\rho_1^n}{1+R_x v_2^{n+1}} \tag{35}$$

When v is set equal to zero in the momentum equation, that equation reduces to $\frac{\partial p}{\partial x} = 0$.

Therefore, the boundary condition becomes

$$p_1^{n+1} = p_2^{n+1} \tag{36}$$

The energy equation with v = 0 becomes

$$\frac{\partial U}{\partial t} + \frac{P}{\rho}\frac{\partial v}{\partial x} = \dot{Q} \tag{37}$$

Equation (37) is written in finite difference form and is used to obtain the energy at the closed end

$$U_1^{n+1} = U_1^n - R_x \frac{p_1^{n+1}}{\rho_1^{n+1}} v_2^{n+1} + \dot{Q}_1^n \tag{38}$$

6.3 Outlet Boundary, v>0

At an outlet boundary, only one quantity can be prescribed for the differential equations. However, the LW and AGM schemes both require one more boundary condition than the differential equations require. The extra boundary condition chosen here is obtained by

linearly extrapolating to the boundary the two values of internal energy at the two nodes next to the boundary. Hence, this boundary condition may be written as

$$U_r^{n+1} = 2U_{r-1}^{n+1} - U_{r-2}^{n+1} \tag{39}$$

which is equivalent to setting the second derivative of energy equal to zero at the boundary. The pressure

$$P_r^{n+1} = P0\ (t^{n+1}) \tag{40}$$

is specified at the outlet.

The velocity at the outlet can be determined from the ρv product in the momentum equation and from the density in the continuity equation at the boundary. The form of the momentum equation used is

$$(\rho v)_r^{n+1} = (\rho v)_r^n - R_x \left[(\rho v^2)_r^{n+1} - (\rho v^2)_{r-1}^n\right] - R_x \left[P_r^{n+1} - P_{r-1}^{n+1}\right] - \Delta t\ F_r^n \tag{41}$$

The density at the outlet is determined from the continuity equation at the outlet with a nonsymmetric space derivative

$$\rho_r^{n+1} = \rho_r^n - R_x \left[(\rho v)_r^{n+1} - (\rho v)_{r-1}^{n+1}\right] \tag{42}$$

Then the new velocity is computed from

$$V_r^{n+1} = \frac{(\rho v)_r^{n+1}}{\rho_r^{n+1}} \tag{43}$$

6.4 Flow Reversal at an Outflow Boundary

When flow reverses at a boundary which was initially prescribed to be an outflow boundary, the prescribed pressure boundary condition continues to be prescribed. However, the internal energy at an inflow boundary that was previously at the outflow boundary becomes prescribed as the internal energy from the previous time step as

$$U_r^{n+1} = U_r^n \tag{44}$$

7. STABILITY ANALYSES OF THE ALTERNATING GRADIENT METHOD

A linear stability analysis can be performed to determine the stability restrictions on the AGM scheme by neglecting the source terms and making the approximation

$$\frac{\partial F(V)}{\partial x} = A\frac{\partial V}{\partial x} \tag{45}$$

where A is a constant matrix which is an approximation to the Jacobian of F(V) with respect to V. The predictor and corrector equations for these assumptions become, respectively,

$$\hat{V}^{n+1}_{j+\frac{1}{2}} = \frac{1}{2}\left(V^n_{j+1} + V^n_j\right) - \frac{\Delta t}{\Delta x} A \left(V^n_{j+1} - V^n_j\right) \tag{46}$$

$$V^{n+1}_j = V^n_j - \frac{\Delta t}{\Delta x} A \left(\hat{V}^{n+1}_{j+\frac{1}{2}} - \hat{V}^{n+1}_{j-\frac{1}{2}}\right) \tag{47}$$

A combined equation may be obtained as

$$V^{n+1}_j = V^n_j - \frac{\Delta t}{\Delta x} A \left[\frac{1}{2}\left(V^n_{j+1} - V^n_{j-1}\right)\right] + \left(\frac{\Delta t}{\Delta x} A\right)^2 \left(V^n_{j+1} - 2V^n_j + V^n_{j-1}\right) \tag{48}$$

The amplification matrix for the propagation of errors generated at a given time is obtained in a manner similar to that presented

in Richtmyer and Morton (1967, p 303). The amplification matrix is

$$G = I - i \frac{\Delta t}{\Delta x} A \sin \alpha - 2 \left(\frac{\Delta t}{\Delta x} A\right)^2 (1 - \cos \alpha) \tag{49}$$

where α is a parameter. If λ is an eigenvalue of the matrix A, then the corresponding eigenvalue of G is

$$g = 1 - i \frac{\Delta t}{\Delta x} \lambda \sin \alpha - 2\left(\frac{\Delta t}{\Delta x}\lambda\right)^2 (1 - \cos \alpha) \tag{50}$$

A stable numerical scheme requires that $|g| \leq 1$. The value of g for the alternating gradient method is most easily obtained by first obtaining the value of g for the two-step Lax-Wendroff scheme, g_{LW}, which is

$$g_{LW} = 1 - \left(\frac{\Delta t}{\Delta x}\lambda\right)^2 + \left(\frac{\Delta t}{\Delta x}\lambda\right)^2 \cos \alpha - i \frac{\Delta t}{\Delta x}\lambda \sin \alpha \tag{51}$$

The graph of this equation is an ellipse centered at $1 - \left(\frac{\Delta t}{\Delta x}\lambda\right)^2$ with major and minor axes of $\left(\frac{\Delta t}{\Delta x}\lambda\right)^2$ and $\left(\frac{\Delta t}{\Delta x}\lambda\right)$. The value of $|g|_{LW}$ is

$$|g_{LW}| = \sqrt{\left|1 - \left(\lambda\frac{\Delta t}{\Delta x}\right)^2 (1 - \cos \alpha)\right|^2 + \left(\lambda\frac{\Delta t}{\Delta x}\right)^2 \sin^2\alpha} \tag{52}$$

For a given value of $|g_{LW}|$, the extrema are determined by setting the derivative of $|g_{LW}|$ equal to zero. The two roots of the resulting equation are $\sin \alpha = 0$ and $\cos \alpha = 1$. The values of g_{LW} for these extrema are given by

$$\alpha = 0 \; ; \; |g_{LW}| = 1 \tag{53}$$

$$\alpha = \pi \quad ; \quad |g_{LW}| = \sqrt{\left|1 - 2(\lambda\frac{\Delta t}{\Delta x})^2\right|^2} \tag{54}$$

Thus, the LW method is conditionally stable because the value of $|g_{LW}| \leq 1$ if $\lambda \frac{\Delta t}{\Delta x} \leq 1$.

For the alternating gradient method, the value of $|g|$ is always less than or equal to $|g_{LW}|$ if

$$2\,(\lambda\frac{\Delta t}{\Delta x})^2_{AGM} = (\lambda\frac{\Delta t}{\Delta x})^2 \tag{55}$$

When this condition is satisifed, the graph of g is seen to be an ellipse which is contained within the Lax-Wendroff ellipse. The real axis of the ellipse is equal to the real axis of the Lax-Wendroff ellipse and the imaginary axis is smaller. Therfore the stability restriction for the AGM is given by

$$2\,(\lambda\frac{\Delta t}{\Delta x})^2 \leq 1 \tag{56}$$

The eigenvalues of the matrix A are given by

$$\lambda = v \text{ and } v \pm c \tag{57}$$

where c is the speed of sound (Richtmyer and Morton, 1967, p 304). Consequently, the stability restriction on the alternating gradient method obtained by combining Equations (56) and (57) is

$$(|v| + c)\frac{\Delta t}{\Delta x} \leq \frac{1}{\sqrt{2}} \tag{58}$$

8. TRUNCATION ERROR OF THE AGM AND LW SCHEMES

The consistency and convergence of the AGM and LW schemes can be proven by showing that the Taylor series truncation error approaches zero as the increment sizes are decreased to zero. The Taylor series truncation error E_T is defined as

$$E_T = \left| L(V) - \mathcal{L}(V) \right| \tag{59}$$

where L is the finite difference operator and $\mathcal{L}$ is the differential operator. Substitution of the linearized forms of the difference and differential equations into Equation (59) yields

$$E_T = \left| \frac{V_i^{n+1} - V_j^n}{\Delta t} - \frac{A}{2\Delta x}(V_{j+1}^n - V_{j-1}^n) + \Delta t \left(\frac{A}{\Delta x}\right)^2 (V_{j+1}^n - 2V_j^n + V_{j-1}^n) \right.$$

$$\left. - G_j^n + \frac{A}{2\Delta x}(G_{j+1}^n - G_{j-1}^n) - \left(\frac{\partial V}{\partial t} - A\frac{\partial V}{\partial x} - G\right) \right| \tag{60}$$

If all quantities are expanded about the point (n,j) then the truncation error becomes

$$E_T = \left| \frac{\Delta t}{2!}\frac{\partial^2 V}{\partial t^2} + A\frac{\Delta x^2}{3!}\frac{\partial^3 V}{\partial x^3} - \Delta t\, A\frac{\partial^2 V}{\partial x^2} - \Delta t\, A\frac{\partial G}{\partial x} \right| + \mathcal{O}(\Delta t^2, \Delta x^4) \tag{61}$$

where $\mathcal{O}$ designates terms of the indicated order and higher. In the instance for which G = 0, the truncation error becomes

$$E_T = \left| A\frac{\Delta x^2}{3!}\frac{\partial^3 V}{\partial x^3} - \frac{\Delta t}{2} A\frac{\partial^2 V}{\partial x^2} \right| + \mathcal{O}(\Delta t^2, \Delta x^4) \tag{62}$$

The second term in parentheses in Equation (62) cancels completely for the two-step Lax-Wendroff scheme (only when G=0). Hence, the Lax-Wendroff scheme is more nearly accurate than the alternating gradient method. Since the truncation error approaches zero as Δt and Δx approach zero, both methods are consistent and convergent.

9. RESULTS OF COMPUTATIONS

Three solutions obtained with the alternating gradient method are presented in this section. The first two are compared with analytical solutions and the last is compared with experimental data. The numerical results presented are all converged values (that is, a small enough time and distance step was selected to insure that the results will not change in the third significant figure if a smaller step is taken).

9.1 Ideal Gas Shock Tube

The capability of a finite difference scheme to solve gas shock tube problems tests only the internal finite difference scheme. Boundary conditions are not used until the shock front reaches the boundary. Results were obtained from both the LW and AGM schemes in order to compare these two methods in the interior.

The problem run is for a 7.8-to-1 initial pressure ratio at the middle of a 20-ft-long pipe. The pressure to the left of the middle is 114.7 psia and to the right it is 14.7 psia. The velocity is uniformly zero and the internal energy is uniformly 80.62 Btu/lbm initially. A diatomic gas having a specific heat ratio of 1.4 was used. No friction or artificial viscosity was employed except for the artificial viscosity inherent in the numerical schemes. The time step size was 0.1 msec, and 60 nodes were used.

The analytical solution for this problem is

$$u = \begin{cases} (1)\ u_i \quad 0 \le x \le 10 - 1120t \\ (2)\ \text{Rarefaction wave for} \\ \quad 10 - 1120t \le x \le 10 - (1120 \cdot \sqrt{.7271} - 820)t \\ (3)\ u_c \text{ for} \\ \quad 10 - (1120 \cdot \sqrt{.7271} - 820)\ t \le x \le 10 + 820t \\ (4)\ u_s \text{ for } 10 + 820t \le x \le 10 + 1710\,t \\ (5)\ u_f \text{ for } 10 + 1710t \le x \le 20 \end{cases} \tag{63}$$

where t is in sec and x is in ft.

The vector U is composed of three components

$$U = (v, P, C)$$

Where C is the sound speed in ft/sec, v is in ft/sec, and P is in psia.

$$v_i = 0, \quad P_i = 114.7, \quad C_i = 1120$$

$$v_c = 820, \quad P_c = 37.6, \quad C_c = 955$$

$$v_s = 820, \quad P_s = 37.6, \quad C_s = 1290$$

$$v_f = 0, \quad P_f = 14.7, \quad C_f = 1120$$

Results at five milliseconds from the alternating gradient method, the two-step Lax-Wendroff method, and the analytical solution are presented in Figure 3. The alternating gradient method completely damps out the large oscillation at the shock front much better than the Lax-Wendroff scheme. The oscillation at the initial contact surface is larger with the two-step Lax-Wendroff method than with the alternating gradient method. The reason that the AGM exhibits smaller oscillations than the LW scheme is due to the larger numerical damping in the AGM than in the LW method.

9.2 Blowdown of Ideal Gas

Results for the blowdown of an ideal diatomic gas with a heat capacity ratio of 1.4 are given in Figures 4 and 5. Figure 4 is a plot of the pressure, P, at the closed end vs time. The numerical results obtained with the AGM are compared with an analytical wave diagram solution obtained from Rudinger (1969, p 192). The pipe length is 13 ft and the ratio of the initial pressure in the pipe to the ambient pressure is 2.83. The initial pressure is 1000 psia. As can be seen, the agreement is generally good. For example, the analytical solution produces a relative minimum of 106 psia at about 22 milliseconds and a relative maximum of 544 psia at about 34

milliseconds which is matched quite well by the AGM values of 109.8 and 554.9, respectively. The time at which the relative maximum occurs for the AGM results differs by about two milliseconds from the analytical solution.

The calculated velocity results at the break are presented in Figure 5. The fluid reverses direction at about 18 msec. Insufficient points are

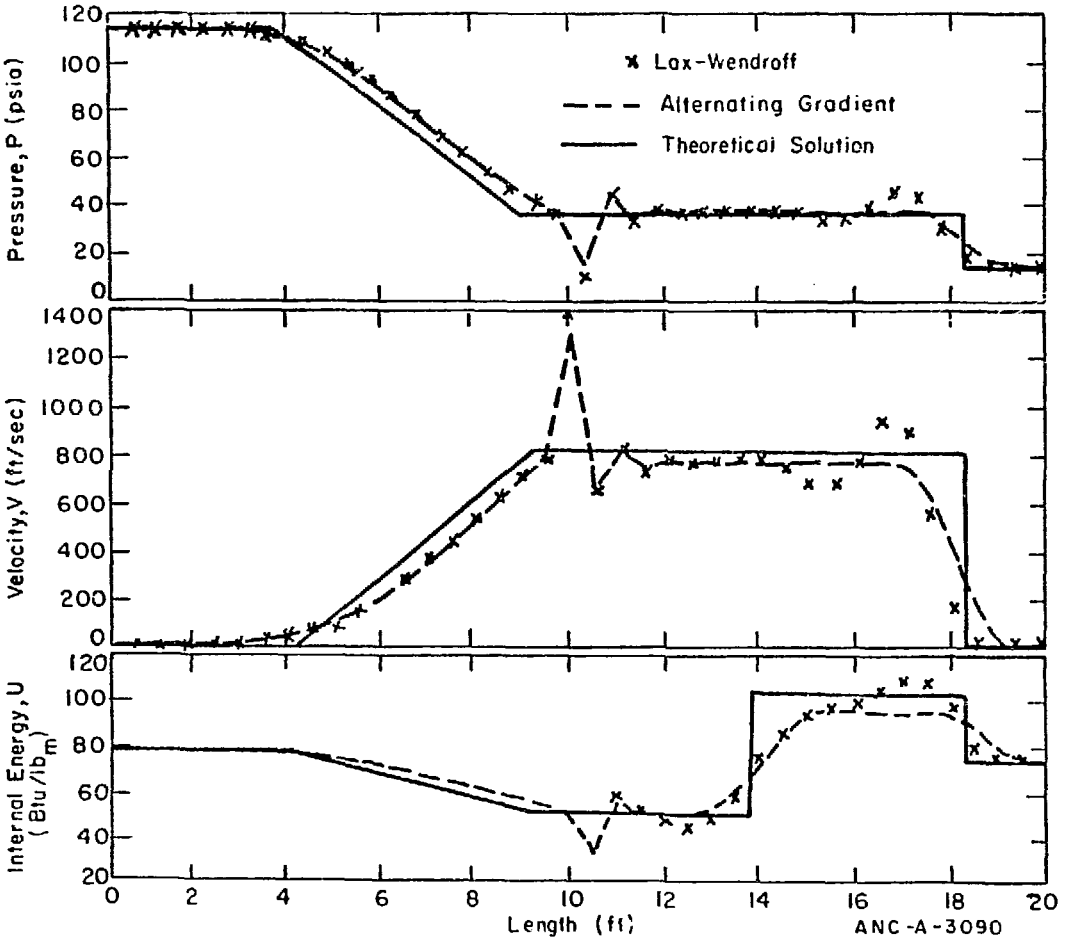

Figure 3. Comparison of the Lax-Wendroff and Alternating Gradient Methods with the Theoretical Solution (time = 5 msec) 60 volumes, Δt = 0.1 msec

presented by Rudinger (1969) to construct an accurate velocity graph. However, enough information is presented by Rudinger to show that the first maximum analytical value is 1405 ft/sec and the first minimun analytical value is -720 ft/sec. The AGM values in Figure 5 agree well with Rudinger's values.

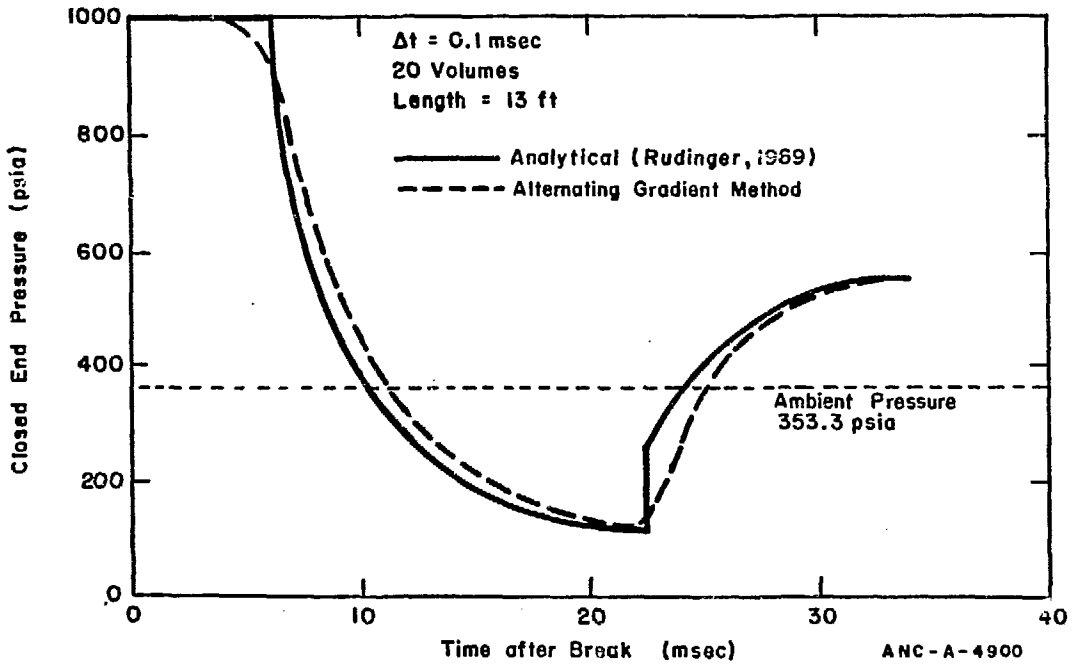

Figure 4. Ideal Gas Blowdown Pressure Results
Δt = 0.1 msec

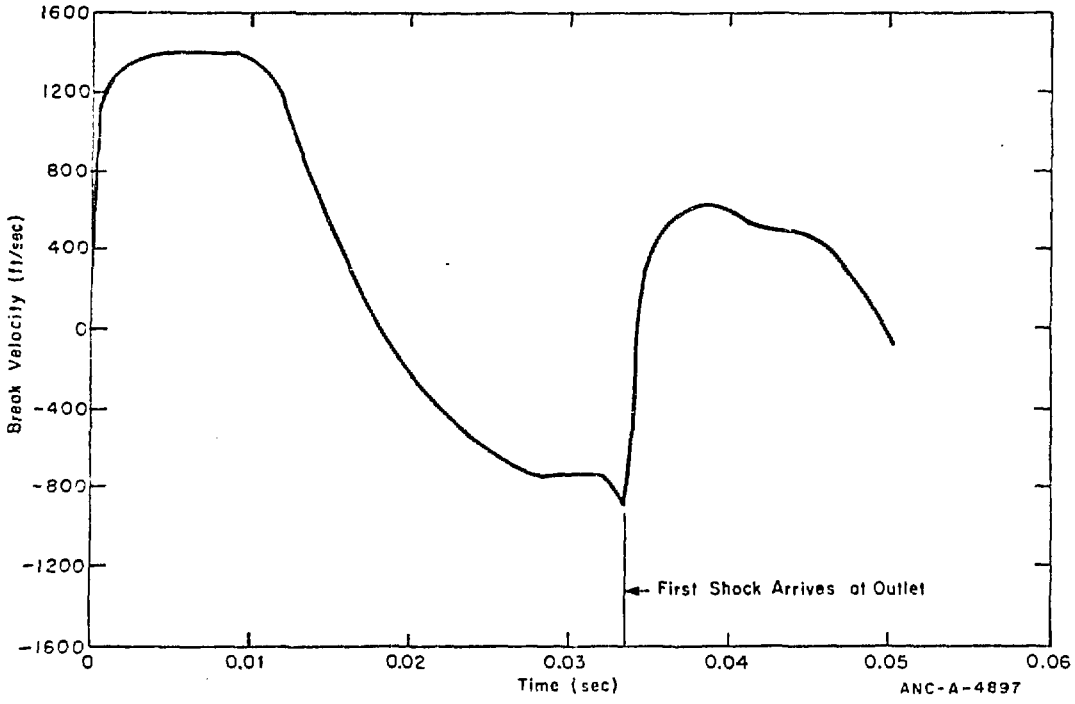

Figure 5. Ideal Gas Blowdown Velocity Results (20 volumes, Δt = 0.4 msec)

The boundary condition at the outlet for pressure and energy were specified when the flow reversed as follows. The relation for the pressure resulting from an adiabatic compression of an ideal gas is (Shapiro, 1953).

$$P = \frac{P_o}{\left[1 + \frac{k-1}{2} M^2\right]^{k/(k-1)}} \tag{64}$$

where P_o = stagnation pressure = 353.3 psia

and $M = \frac{v}{C_o}$

k = heat capacity ratio = 1.4

and C_o = stagnation sound speed = 1755 ft/sec

This boundary condition ensures that fluid is drawn into the pipe isentropically from the stagnation pressure. This treatment is necessary to assure that the analytical solution presented by Rudinger (1969) and the AGM solution are solutions to the same problem.

Equation (64) was programmed and used at the exit when the velocity reversed as

$$P_r^{n+1} = \frac{353.3}{\left[1 + 0.2\frac{(v_r^{n+1})^2}{C_o}\right]^{3.5}} \tag{65}$$

The energy, U_r^{n+1}, becomes prescribed to be the stagnation value as

$$U_r^{n+1} = U0 = 296.26 \text{ Btu/lbm.} \tag{66}$$

The density is computed from the equation of state. The velocity is computed from the same boundary condition as used before flow reverses.

9.3 Blowdown of a Steam-Water Mixture

Results are given in Figures 6 to 8 for an experimental blowdown of a steam-water mixture from a pipe 13.44 ft long and 0.24 ft in diameter with one end open (Edwards and O'Brien, 1970). This particular experiment is currently used in the nuclear industry as a standard against which to check computational models. The initial pressure is 1000 psig and temperature is 465°F. These initial conditions correspond to subcooled water conditions.

Short term pressure transient plots are presented in Figure 6 for two measurement stations. Results computed using the alternating gradient method are compared with results from Experimental Runs 51 through 53 from Edwards and O'Brien (1970). The three experimental runs are attempts to repeat the same experiment. Twenty uniform finite difference nodes and a uniform time step size of 0.1 msec were used. No choking correlation or two-phase friction multipliers were used. The viscosity required in the Reynolds number in the friction factor was obtained by using the void fraction as a weighting factor. The smooth pipe friction factor was used (Knudsen and Katz, 1958). The steam-water properties are based on the 1967 ASME steam tables (Meyer et al., 1967). The pressure at the break was computed as

$$p_r^{n+1} = \frac{p_{r-1}^{n+1} + 14.7 \text{ psia}}{2} \tag{67}$$

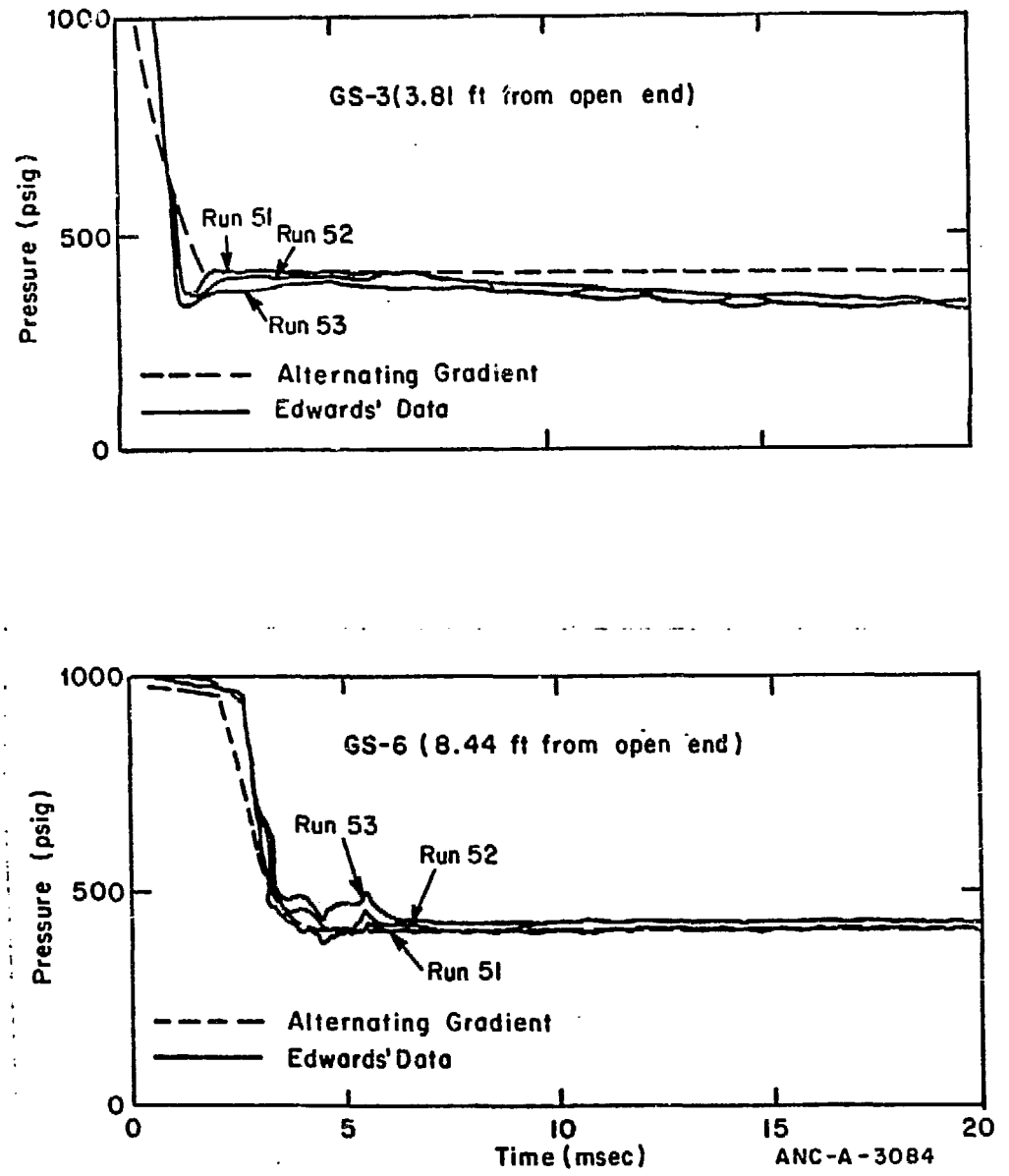

Figure 6. Comparison of Alternating Gradient Short Term Pressure Transient Computations with Edwards' Data. 20 Volumes, Δt = 0.1 msec

As can be seen, the agreement is excellent (Figure 6). The long term pressure transients for the same two measurements are presented in Figure 7. Again, agreement between code results and Edwards and O'Brien (1970) data is excellent. The long term void fraction transient results are compared with experiment results at the middle of the pipe in Figure 8. The agreement is fair.

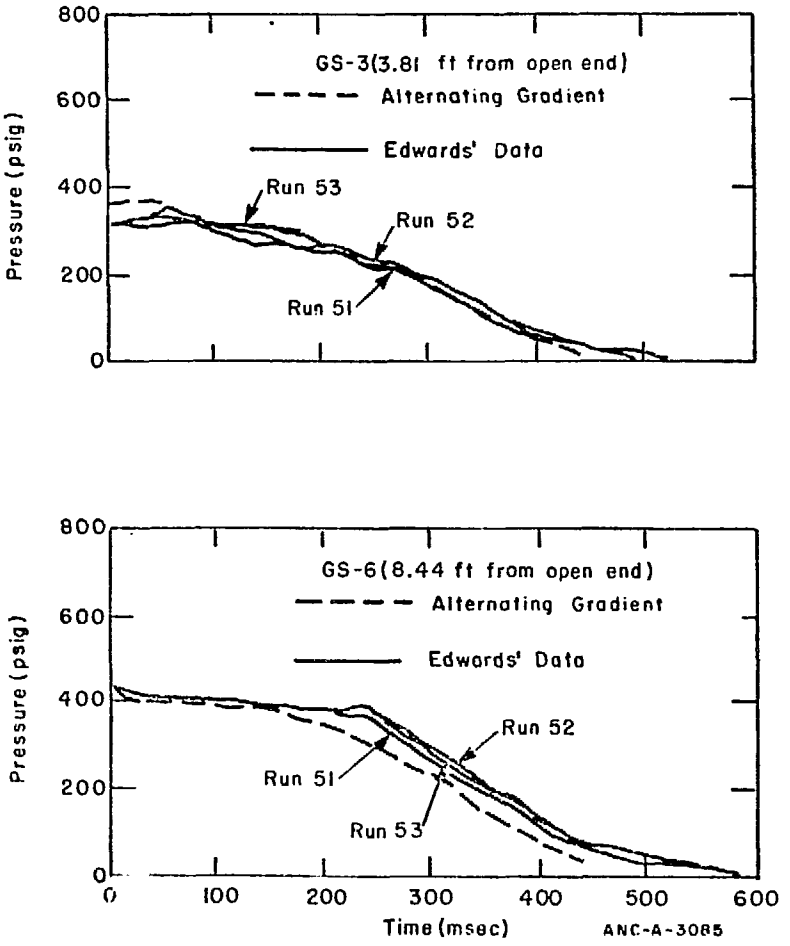

Figure 7. Comparison of Alternating Gradient Long Term Pressure Transient Response Computations with Edwards' Data. 20 Volumes, Δt = 0.1 msec

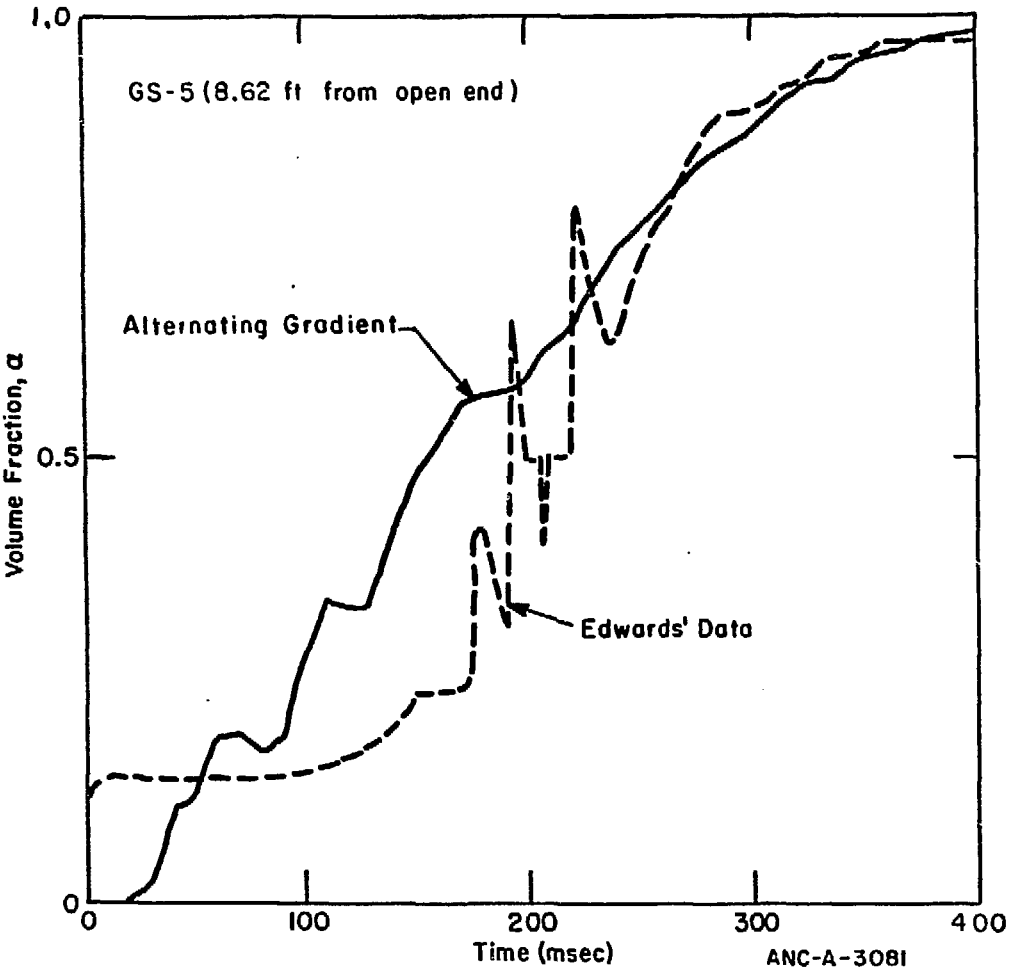

Figure 8. Comparisons of Alternating Gradient Code Results with Edwards' Data for Volume Fraction Steam Transient. 20 Volumes, Δt = 0.1 msec

The time-step stability restriction for the alternating gradient method given in Equation (58) was verified by varying the time-step size used in this blowdown problem. The initial sound speed in the liquid is 4000 ft/sec. For a 20-volume problem, the AGM stability criterion for the initial pressure wave allows a maximum time-step size of 0.12 msec. The first run with a 0.1-millisecond time-step was stable and predicted well the short term results for the Edwards' experiment. Succeeding runs at 0.15 millisecond and larger time-steps were all unstable. No attempt has been made to increase the time-step size after the initial depressurization when the two-phase sound speed is greatly reduced. After the initial depressurization, the time-step size could be increased to about 2 milliseconds without exceeding the AGM stability criterion.

10. CONCLUSIONS

Comparison of the alternating gradient method and the two-step Lax-Wendroff for the shock tube indicates that the alternating gradient method is more nearly accurate than the Lax-Wendroff scheme probably due to more numerical damping in the AGM. The results obtained with the AGM for the blowdown of a perfect gas from a pipe agreed well with the analytical solution. The calculation of blowdown of a steam-water mixture from a pipe is in as good agreement with experimental data as results from any calculational method even though no correlation was used for choking loss coefficients or two-phase friction multipliers. Although the alternating gradient method is restricted by a time-step limitation which is slightly smaller than the standard Courant condition (Equation 3) for a given time-step and mesh size, it is at least as accurate as implicit schemes. Since only two cycles per time-step are needed, the alternating gradient method is nearly an order of magnitude faster than a fully implicit scheme is for blowdown of a steam-water mixture. The AGM time-step size is not considered a serious limitation for steam-water blowdown analyses and other fast transients, when the maximum velocity, v_{max}, approaches sonic. In this case, the accuracy restriction of an implicit scheme given in Equation (4) is almost the same as the Courant condition. Therefore, for fast transients, implicit schemes have the same restriction as explicit schemes. However, for slow transients for which flashing does not occur (or takes a very long time to occur) the AGM and other explicit methods require a prohibitively small time-step, as compared to implicit numerical schemes.

In addition to the fast running time advantage for fast transients, other advantages of the alternating gradient method are:

1) Averaging errors associated with displaced mesh schemes in calculating spatial gradients of products are eliminated with use of the AGM because all quantities are defined at the same points.
2) Since the AGM is an explicit scheme, matrices need not be inverted as is required with an implicit scheme.
3) It is simple to program.

11. REFERENCES

Chen, J. H., "Numerical Boundary Conditions and Computational Modes", J. Comp. Phys., 13, pp 522-535 (1973).

Chu, C. K. and Sereny, A., "Boundary Conditions in Finite Difference Fluid Dynamic Codes", J. Comp. Phys., 15, pp 426-491 (1974).

Edwards, A. R., and O'Brien, T. P., "Studies of Phenomena Connected with the Depressurization of Water Reactors", J. British Nuc. Energy Soc., 9 pp 125-135 (April 1970).

Knudson, J. G. and Katz, D. L., Fluid Dynamics and Heat Transfer, McGraw Hill, New York (1958).

Lax, P. D., "Weak Solutions of Nonlinear Hyperbolic Equations and Their Numerical Computation", Comm. Pure and Appl. Math., 7, pp 159-193 (1954).

Matsuno, T., "False Reflection of Waves at the Boundary Due to the Use of Finite Differences", J. Met Soc. of Japan, 44, pp 145-157 (1966).

Meyer, C. A., McClintock, R.B., Selvestri, G. J. and Spencer, R. C., Jr., 1967 ASME Steam Tables - Thermodynamic and Transport Properties, New York: The American Society of Mechanical Engineers (1967).

Moore, K. V. and Rettig, W. H., RELAP4-A Computer Program for Transient Thermal-Hydraulic Analysis, Aerojet Nuclear Company Report ANCR-1127 (December, 1973).

Nitta, T., "The Outflow Boundary Condition in Numerical Time Integration of Advective Equations", J. Met. Soc. of Japan, 40, pp 13-24 (1962).

Porsching, T. A., Murphy, J. H. and Redfield, J. A., "Stable Numerical Integration of Conservation Equations for Hydraulic Networks", Nucl. Science and Eng., 43, pp 218-225 (February 1971).

Richtmyer, R. D. and Morton, K. W., Difference Methods for Initial-Value Problems, Interscience, New York (1967).

Roach, P. J., Computational Fluid Dynamics, Hermosa Publishers, Albuquerque (1972).

Rudinger, George, Nonsteady Duct Flow, Dover Publications, Inc., New York (1969), pp 186-195.

Shapiro, A. H., The Dynamics and Thermodynamics of Compressible Fluid Flow, Vol. I, Ronald Press Co., New York (1953), p 83.